# A New Design of a Geothermal Thermoelectric Generator System for Geothermal Heat Recovery

Abdullah Alharb[1]*, Alaa Attar[2]

1-King Abdelaziz University, Rabigh (Kingdom of Saudi Arabia)

2-King Abdelaziz University, Rabigh (Kingdom of Saudi Arabia)


*Corresponding author:


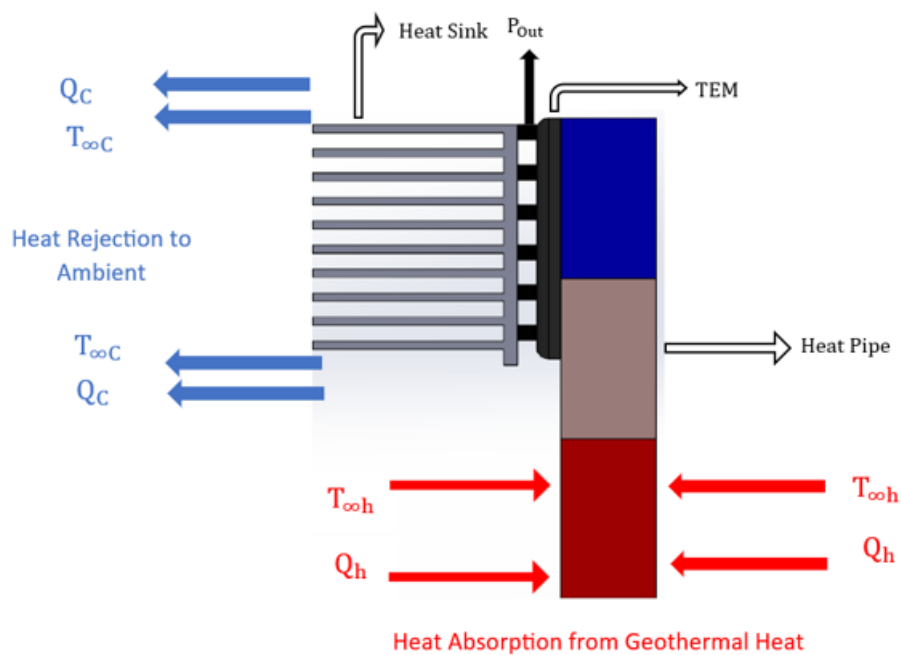Email:AALHARBI2283@stu.kau.edu.sa, Tel: +966595732022

**Graphical Abstract**



**Figure 1: Schematic Diagram of GTEG System**

**Abstract**

The current paper shows the analytical study of a new design of a geothermal thermoelectric generator system (GTEG). Many developments have been made in the

global energy sector in the last few decades, but fossils fuels remained dominant and hold 78.5% global energy demand and are accountable for 75% of global CO2 emissions. Furthermore, geothermal energy has advantages compared to others of weather independence. It has been known and recommended that; the thermoelectric module is a potential technology advancement to accelerate the developments in geothermal power. This study work presents the analytical modelling of the geothermal thermoelectric generator system (GTEG) to study the effect of heat sink, heat pipe, electrical load resistance, and number of thermoelements, to achieve the possible maximum output electrical power. The maximum output power can be reached by optimizing the mentioned parameters where a lower value of thermal resistance of the heat exchangers are needed. Then, the proposed design of the GTEG system is implemented in a location where the geothermal temperature is 157 ℃, and 17 ℃ is the ambient temperature. As a result, and by using natural convection heat sink, the optimum output power density obtained from the GTEG system is 0.235 W/cm².


**Keywords:** (Thermoelectric, Geothermal, Thermoelectric Generator, Heat Pipe, Geothermal Heat Recovery, and Geothermal Thermoelectric Generator System)

## 1. Introduction:

Many developments have been made in the global energy sector in the last few decades, but fossils fuels remained dominant and hold 78.5% global energy demand and are accountable for 75% of global CO2 emissions. Thus, developments regarding this issue in global energy system is highly imperative, to prohibit emissions which are

contributing to climate changes and affecting energy independent countries. For that matter, all renewable resources must be considered because a combination of all these resources might be helpful in obtaining the desired objectives [1].The largest renewable source, geothermal energy has advantage, compared to others, of weather independence, and has a permanence with a great potential. Additionally, it has applications of heating cooling and can be used for power production. However, it still has very little contribution in the global energy sector particularly for power production, of global demands of less than 0.4% [1]. However, the principle of thermoelectric module (TEM) is to convert the temperature difference between the two sides of the TEM into either electrical power or electrical current. TEM uses for either power generation or heating and cooling purposes. Further, TEM is a direct solid-state device that their parts do not move and do not required any intermediate fluid in order to operate and that will reduce the mechanical failure. However, as long as a temperature difference occurs, TE devices will be able to generate power, heating, and cooling. To accelerate the developments in geothermal power, the thermoelectric generator (TEG) are acknowledged as one of the technologies that can be helpful [2]. Therefore, there are huge amount of geothermal energy are existing in the ground and reachable, that is could assist in producing power by using the geothermal wasted heat as this considered as one of the areas of research that people concentrate at is producing power from the geothermal wasted heat using thermoelectric generator. However, this research aims to study the different design of thermoelectric generator to generate electrical power from the geothermal wasted heat. Furthermore, for geothermal energy recovery process, Catalan et al. [3] have developed the initial geothermal thermoelectric generator (GTEG) Consist of thermoelectric generator and phase change heat exchanger attached to the hot side of the module. This enabled them to incorporate thermoelectricity into

the entire generator, resulting in a completely passive device devoid of moving parts and auxiliary consumption. In the last years, the combination of thermoelectric generators and phase change heat exchangers take an advantage of the latent heat of internal fluids which condense and vaporize cyclically in order to transfer heat over long distances which could lead to low thermal resistances and these heat exchangers were used in several applications. Therefore, Catalan et al. [1], presented a GTEG suitability with a passive phase change heat exchanger. The device was able to produce more than 520 kWh of energy. The installed equipment for power generation had two prototypes, where the first prototype consists of 10 modules of 5 levels stands 1m above ground, while the second one involves 6 thermoelectric modules of 3 levels and placed 0.85m above the ground, it was concluded and confirmed that, although a total generation of power could be higher, but installation of higher number of modules lead to decrease in the generation power per module. As the 10 thermoelectric modules prototype produced 20.9W with the temperature difference of 158°C, and the other prototype which consists of 6 modules produced 16.67W under the same specifications. Moreover, these results were presented for the large-scale application with the advantage of modularity, strength, reliability, and slight environmental effect of equipment. In addition, Alegria et al. [4], have studied a unique geothermal TEG device which was developed with varying biphasic heat exchanger configurations. The objective is to obtain low thermal resistance to maximize the efficiency of the thermoelectric modules. Thus, a strong, and passive heat exchanger can be achieved with 0.07K/W and 0.4K/W thermal resistances for the hot and cold sides respectively. The GTEG system constructed with efficient and effective heat exchangers system, as it experimentally generated 36W with a temperature difference of 160°C between the hot and cold temperature sources. Moreover, this study concluded and shown that, it is

possible to increase power production with compacting more generators, as a smaller number of modules (from 10 to 6) could increase the efficiency from 3.72%-4.06%.

On the other hand, for low temperatures use, Ahiska et al. [5], implemented a design of a portable TEG of 100W for low geothermal temperatures using a special software which been developed and used for the first time. This report evaluated the effect of hot and cold-water flow rate, and temperature difference between surfaces. It also studied the effect of the load resistance as it has an influence on power output and TEG efficiencies. It was concluded that, the hot–cold water flow that passed throughout the surfaces of the TEG were improved by up to 3.7-12.8 l/min, under a temperature difference of 67°C. Moreover, the maximum output power of the TEG was obtained as 41.6W with a conversion efficiency of 3.9% when the load resistance of the TEG was almost 15 Ω. Alegría et al. [6], developed a computational model of GTEG which was used for the first time for estimating the generated electrical power in Lanzarote as it worked as a tool to design and optimize thermoelectric generators. The model was proven with the results of two TEG installed in two different areas and was able to achieve a relative error of less than 10% while predicting the power, and between 0.5–1.6% in the annual power production. Furthermore, Gavin Newsom [7] aimed to develop a TEG device in northern California which could help in producing electricity by using a geothermal heat as an input source to the system. So, a GTEG system was built and designed to have a maximum power generation by increasing the number of layers. Moreover, the device was tested and resulted that, a 6-layer TEG field-scale device generated 500W power with 152°C temperature difference between hot and cold sources. Finally, the study showed and concluded that, a GTEG system could produce electrical power in a wide competitive and economic range as compared to solar PV panels when external factors such as capacity factor are considered. Designing and

optimizing a thermoelectric generator system has been challenged, Bass et al. [8] in 1994 established a developed thermoelectric generator system to use it for a diesel truck engine, with the aim of generating 1 Kw as an output from the system. In this system, 72 TE modules were used which produced an output electrical power of 1068W. It was also reported that the best thermoelectric material is bismuth telluride (Bi2Te3) for exhaust waste heat applications because of very efficient performance regardless the temperature of maximum operating temperature. Moreover, this technology could also be used in exhaust gas and water circulation systems. As the study performed by Birkholz et al. [9] demonstrated on the prototype which been developed by porch company in 1988, they developed it in order to test a thermoelectric generator module (TEG) by using both, the exhaust gas and water circulation systems. The thermoelectric material which was used in that test was iron silicide (FeSi2), which was connected to the company engine Porsche 944. The difference of temperature between both the hot and cold side of the TE module was 490 Kelvin, while the achieved output power was 58 W for 90 thermoelements. Similarly, Attar et al. [10] studied the optimal load resistance and geometric ratio of a thermoelectric generator module, which were determined simultaneously using an analytical approach with dimensional analysis. The configurations were adjusted to maximize the output power of the TEG that connected to two heat sinks. The comprehensive investigation has both theoretical and experimental approaches which demonstrated that, in order to obtain the maximum output power of the module, the temperature difference between the hot and cold sides of the module must be constant, which is difficult to occur in real applications of the thermoelectric module. Another challenging matter is related to the thermoelectric module (TEM), as designers facing challenges while obtaining the actual intrinsic material property of the TEM as these material properties are very important to avoid

6

the effective Thomson effect and electrical and thermal contact resistances which could affect the output power. Weera et al. [11] evaluated the efficiency of a commercial TEM performance. The performance of the commercial TEM was compared to that of the experimental testing. In order to calculate the effective material properties, the maximum parameters which given by the module manufacturer can be used. The efficiency of these material properties technique is supported by both commercially given data and analytical findings as a tool for predicting the performance of the commercial module. The effective material characteristics, including electrical and thermal contact resistance, have negative impacts on the performance of both TEGs and TECs. In addition, the Thomson effect is a potential factor that can impact the precision of material properties. However, inserting the effective material properties into the ideal equations helps to mitigate losses and uncertainties that may arise when evaluating the performance of TEM using intrinsic material properties. Many efforts been consumed in previous studies related thermoelectric generator system and geothermal thermoelectric generator systems. To continue this journey several areas are able to be developed and improved to increase and optimize the output electrical power. However, a new design was proposed in this research to improve the output power by considering contact resistances. The objective of this research is to study and optimize the analytically combined design of heat pipe, heat sink, and thermoelectric generator module to find out the maximum possible output power. So, this study proposed two different designs the first one with neglecting thermal and electrical contact resistances and the second design will consider both electrical and thermal contact resistances to figure out the optimum value of the leg length in order to improve the first design by obtaining the optimum output electrical power. The GTEG system consists of a TEG which is sandwiched between a Heat Pipe and Heat sink, where the hot side of the

7

system has a heat pipe to absorb the geothermal heat, while a heat sink is attached to the cold side to reject the heat to the ambient. The model is designed to study the effect of heat sink, heat pipe, number of thermoelements, and electrical load resistance in order to achieve the maximum output electrical power. The maximum output power from the GTEG system can be reached by optimizing the mentioned parameters where the minimum thermal resistances of the heat sink and heat pipe are needed as well as both the electrical load resistance and the number of thermoelements of the TE module are optimized simultaneously.

**Table 1: Summary of previous studies related to the thermoelectric generator systems & geothermal thermoelectric generator systems**

| Author | System Type | Material | Number of Modules | Temperature Difference (°C) | Output Power (W) | Conversion Efficiency (%) |
|---|---|---|---|---|---|---|
| Bass et al. [8] | Automotive Waste Heat Recovery | bismuth telluride (Bi2Te3) | 72 | | 1068 | |
| Birkholz et al. [9] | Automotive Waste Heat Recovery | Iron Silicide (FeSi2) | 90 | 217 | 58 | |
| Catalan et al. [1] | GTEG | | 10 — 6 | 158 | 20.67 — 16.67 | |
| Alegria et al. [4] | GTEG | | 10 — 6 | 160 | 17 — 19 | 4.06 |
| Ahiska et al. [5] | GTEG | | 20 | 67 | 41.6 | 3.95 |
| Catalan et al. [3] | GTEG | | 2 | 180 | 3.29 | |

| | | | | | | |
|---|---|---|---|---|---|---|
| Gavin Newsom [7] | GTEG | | 125 | 152 | 500 | |

## 2. Methodology

### 2.1 The proposed analytical design of (GTEG) system

The Proposed design of this system consists of three major components, these components are presented below in figure 1 Which are: the thermoelectric generator module sandwiched between the copper heat pipe and heat sink, the heat pipe will absorb the geothermal heat and deliver it to the second component which will be the TEG, and a heat sink attached to the other side of the module to reject heat to the surrounding.
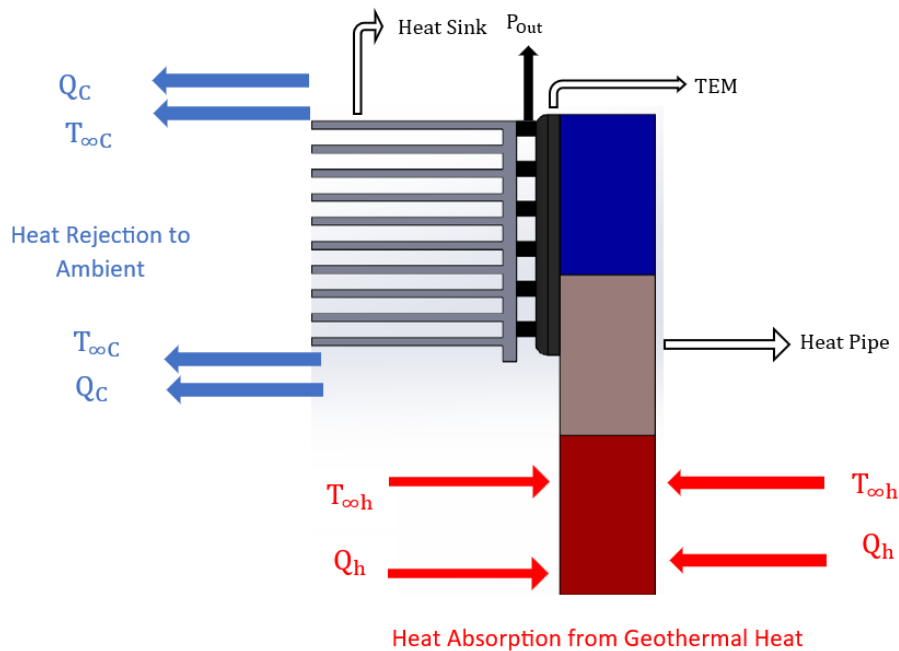


**Figure 1: Schematic diagram of GTEG system**

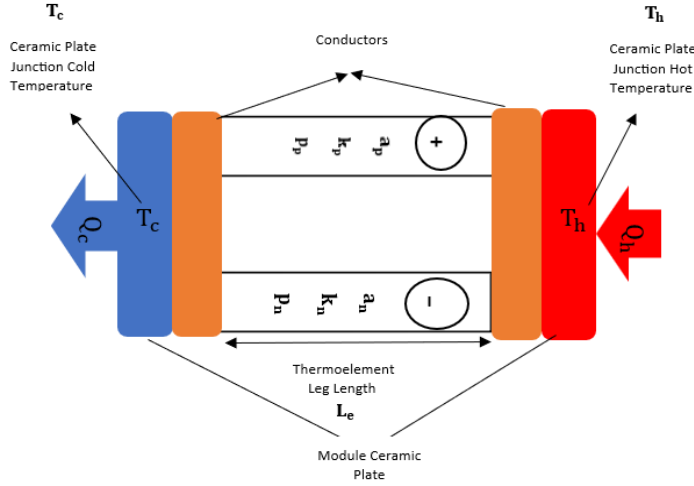## 2.2 The proposed analytical GTEG system neglecting contact resistances (design 1)



**Figure 2: Configuration of a single basic thermoelectric couple neglecting electrical and thermal contact resistances for design 1**

The present GTEG system was designed and modelled analytically using the below four equations where will be explained below from equation (1) – (4).The below governing equation of the current design can be applied with respect to the following assumptions, the flow of heat is at steady state condition, Thomson effect is neglected, the module contact resistances are neglected as shown above in figure 2, and radiation and convection heat transfer through the module are neglected these assumptions and formulation been used by Lee [12].

Hence, the four equations become as follow:

$$Q_h = \frac{(T_{\infty h} - T_h)}{R_{total1}} \tag{1}$$

$$Q_h = n \left[ \alpha_e \frac{\alpha_e(T_h - T_c)}{\frac{R_L}{n} + \frac{\rho_e}{G_e}} T_h - \frac{1}{2} \left[ \frac{\alpha_e(T_h - T_c)}{\frac{R_L}{n} + \frac{\rho_e}{G_e}} \right]^2 \frac{\rho_e}{G_e} + G_e k_e (T_h - T_c) \right] \qquad (2)$$

$$Q_c = n \left[ \alpha_e \frac{\alpha_e(T_h - T_c)}{\frac{R_L}{n} + \frac{\rho_e}{G_e}} T_c + \frac{1}{2} \left[ \frac{\alpha_e(T_h - T_c)}{\frac{R_L}{n} + \frac{\rho_e}{G_e}} \right]^2 \frac{\rho_e}{G_e} + G_e k_e (T_h - T_c) \right] \qquad (3)$$

$$Q_c = \frac{(T_c - T_{\infty c})}{R_{total2}} \qquad (4)$$

$$W_n = Q_h - Q_c \qquad (5)$$

$$\eta_{TE} = \frac{w_n}{Q_h} \qquad (6)$$

$Q_h$, is the input heat into the system which is coming from geothermal energy in (W), while $Q_C$ is the cooling side which is the rejected heat from the system. $T_{\infty h}$ is the hot source temperature, and $T_{\infty c}$ is the ambient temperature. Further, $T_h$ is the temperature of the hot surface of the module, while $T_c$ is the cold one. Respectively, $R_{Total1}$ is the sum of all thermal resistances which occur at the hot sections of the heat pipe while heat is transferring, the term $R_{Total2}$ refers to the total thermal resistances for the cold side the convection conductance of the coolant fluid which represents efficiency of the heat sink, heat coefficient and the heat sink's surface area.

$[\frac{\alpha_e(T_h - T_c)}{\frac{R_L}{n} + \frac{\rho_e}{G_e}}]$, this term is representing the electrical current. The term n represents thermoelements number, the load resistance is defined as $R_L$, and $G_e$ is the geometry ratio which is $(A_e/L_e)$. These three parameters which are provided and can be obtained from the data sheet of the selected module. Moreover, the following three parameters $\alpha_e$, $k_e$ and $\rho_e$ are called effective material properties which will be defined later. All these mention parameters should be calculated using the module input parameters. However, $Q_h$, $Q_C$, $T_h$ and $T_C$ are the four unknown varibals from the governing

equations. Furthermore, equations (5) and (6) should be used to calculate both, the system produced power in (W) and the module's efficiency in (%).

## 2.3 The proposed analytical GTEG system considering contact resistances (design 2)
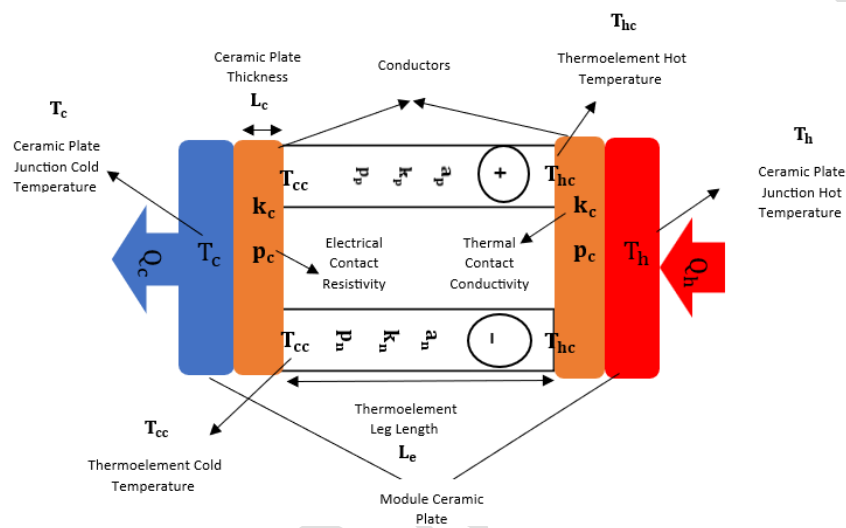


**Figure 3: Configuration of a single thermoelectric couple considering electrical and thermal contact resistances for design 2**

Although the previous discussion referred to the ideal thermoelectric equations which were not included thermal and electrical contact resistances, the practical TE devices require to include of both electrical and thermal contact resistances as shown above in figure 3, which will be the subject matter of this segment. However, in terms of the TEG performance, including these contact resistances will definitely lead to a lower performance specially when it compares to that performance of the ideal equation. The thermocouple consists of p and n type materials which have a series connection with each other as well as sandwiched between two layers of ceramic plates [12]. However, to evaluate the module test, it is necessary to consider both the electrical and thermal

12

contact resistances. Due to the large number of thermocouples containing the module, it is possible to analyze and study a uncouple. Prediction of the module test is possible as it can be calculated using a commercial module's intrinsic properties with the written equations below. Thus, using below method can lead us to find out the optimum thermoelement leg length, then the optimum value of a leg length can be considered and used in our new optimum design which will give the optimum output power.

$$Q_h = \frac{(T_{\infty h} - T_h)}{R_{totalh}} \tag{7}$$

$$Q_h = \frac{Ak_c}{l_c}(T_h - T_{hc}) \tag{8}$$

$$Q_h = \alpha I T_{hc} - \frac{1}{2}I^2 R - \frac{Ak}{l_e}(T_{cc} - T_{hc}) \tag{9}$$

$$Q_c = \alpha I T_{cc} - \frac{1}{2}I^2 R - \frac{Ak}{l_e}(T_{cc} - T_{hc}) \tag{10}$$

$$Q_c = \frac{(T_c - T_{\infty c})}{R_{totalc}} \tag{11}$$

$$Q_c = \frac{Ak_c}{l_c}(T_{cc} - T_c) \tag{12}$$

$$I = \frac{\alpha(T_{hc} - T_{cc})}{R_L + R_e} \tag{13}$$

Where the internal resistance $R_e$ equals to,

$$R_e = \frac{\rho l_e}{A_e} + \frac{\rho c}{A_e} \tag{14}$$

Where, $Q_h$ represents the absorbed heat flow rate at the hot side junction temperature $T_h$, $Q_c$ is the liberated heat flow rate at the cold side junction temperature $T_c$, the element's cross sectional area represented as $A_e$, $k_c$ is the ceramic plate's thermal conductivity, $\rho c$ express the electrical contact resistivity, $L_e$ is the element leg length, $L_c$ is the ceramic plate thickness, $R_L$ represents the load resistance, and $I$ is the electrical current.

However, these above-mentioned equations (7-14) can be used to solve both equations (15) and (16) which represents the hot and cold side thermoelements temperature $T_{hc}$ & $T_{cc}$ as a function of the below six parameters:

$$T_{hc} = T_{hc}\left(R_L, T_h, A_e, I_e, p_c, k_c\right) \qquad (15)$$

$$T_{cc} = T_{cc}\left(R_L, T_h, A_e, I_e, p_c, k_c\right) \qquad (16)$$

By utilizing a mathematical program, it is possible to resolve these two functional equations to calculate $T_{hc}$ & $T_{cc}$ in order to get $Q_h$ and $Q_c$ which represent the rates of heat flow, as well as the efficiency of the thermoelectric module. Using same material and specifications of our proposed TEM, it can be clearly noticed that, the optimum output power occurs with a leg length value of almost 1.8 mm, so this value of optimum leg length will be considered in our optimum design.

### 2.4 Heat sink design

The below shown heat sink in figure 4, plays an important role to significantly improve the functionality of the GTEG system. However, in order to optimize the heat sink and determining the most effective fin spacing and thickness, this part is concentrates on the design of the heat sink. Lee [12] has developed a method to design and optimize the below selected heat sink which can be reject the maximum possible heat from the system. As been mentioned earlier fin thickness and spacing are the two most important parameters while optimizing. Thus, these two parameters were calculated and then optimized using the following equations (17) – (25).
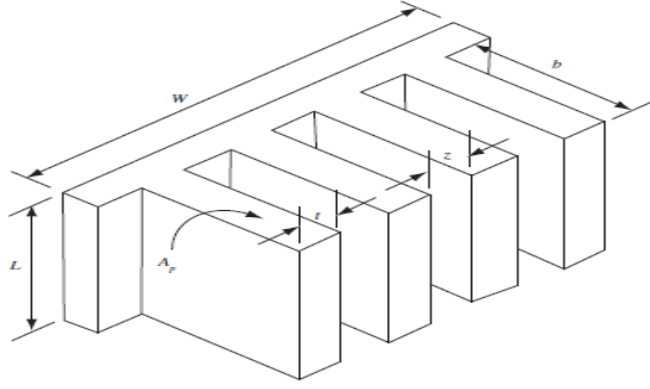
**Figure 4: Multiple fins array heat sink**

Equation (17) represents the heat sink area.

$$A_c = n[2\,(L_s + t_s)b_s + L_s\,z_s] \tag{17}$$

Equation (18) represents the air flow area.

$$A_c = n_s\,b_s\,z_s \tag{18}$$

Equation (19), used to calculate Riyadh number.

$$R_{aL=}\ \frac{g\,\beta(T_{\infty h} - T_{\infty c})\,(L_s{}^3)}{\nu\,\alpha} \tag{19}$$

The below equation (20) uses to calculate the Nusselt number:

$$N_{u=}\quad 0.517\ R_{aL}{}^{1/4} \tag{20}$$

Equation (21), used to calculate the heat coefficient.

$$h = \frac{N_u * k.air}{L_s} \tag{21}$$

Equation (22), used to calculate the single fin efficiency.

$$\eta_s = \frac{\tan_h(m_d\,b_s)}{m_d\,b_s} \tag{22}$$

Where, $m_d = \sqrt{\dfrac{h\,2\,(L_s + t_s)}{k_{alm}\,L_s\ t_s}}$

Equation (23), used to calculate the single fin area.

$$A_f = 2 \ b_s \ (L_s + t_s) \tag{23}$$

Equation (24), used to calculate the total efficiency.

$$\eta_o = 1 - n_f \left(\frac{A_f}{A_t}\right)(1 - \eta_s) \tag{24}$$

Equation (25), used to calculate the optimum fin spacing.

$$Z_{opt} = 3.24 \ R_{aL}^{\frac{-1}{4}} \ P_r^{\frac{-1}{4}} \ L_s \tag{25}$$

### 2.5 Calculation of heat pipe thermal resistances:

As been demonstrated by Lee [12]. It is essential to consider the thermal residences which exist in the heat pipe while designing the system. So, in order to solve the above equation (1), the calculation of the total thermal resistances $R_{total}$ will be defined below.

The total thermal resistances formulated as in equation (26).

$$R_{total} = \ 2\big(R_{w,e} + R_{p,e}\big) \tag{26}$$

The below equation (27) can be used in order to obtain the resistance of the radial conduction resistances for both the evaporator and condenser sections.

Physically $R_{p,e}$ and $R_{p,c}$ are identical as well as $R_{w,e}$ and $R_{w,c}$. Hence,

$$R_{p,e} = R_{p,e} = \frac{\ln \left(\frac{d_o}{d_v}\right)}{2\pi L_e k_p} \tag{27}$$

16

Where, $d_o$, is the outer diameter of the pipe, $d_v$ is the vapor space diameter, the evaporate section lengths is $L_e$, and material thermal conductivity of the heat pipe is $k_p$.

For flat heat pipe, we can replace the above equation with the following equation.

$$R_{p,e} = R_{p,e} = \frac{\delta}{A_e k_p}$$

Where the plate thickness is expressed as $\delta$, and $A_e$ refers to the evaporator section.

In order to obtain the occurred thermal resistances at the wick section, evaporator section, and condenser sections. Equation (18) below can be applied for both $R_{w,e}$ and $R_{w,c}$.

$$R_{w,e} = R_{w,c} = \frac{\ln{(\frac{d_i}{d_v})}}{2\pi L_e k_{eff}} \tag{28}$$

Where, $d_v$, $d_i$ are the vapor section diameter and the pipe's internal diameter, and $k_{eff}$ is the wick screen effective thermal conductivity.

Equation (29) presents the formula of the wick screen effective thermal conductivity.

$$k_{eff} = \frac{k_i[(k_i+k_w)-(1-\varepsilon)(k_i-k_w)}{(k_i+k_w)-(1-\varepsilon)(k_i-k_w)} \tag{29}$$

Where, $\varepsilon$ is the screen wick's porosity, $k_i$ is thermal conductivity of copper, and $k_w$ is thermal conductivity of water.

To obtain the porosity of the wick screen, equation (30) could apply.

$$\varepsilon = 1 - \frac{\pi N d_w}{4} \tag{30}$$

where, $\varepsilon$ is the screen wick's porosity, N is the number of wick mesh number layer, and $d_w$ is the mesh wire diameter.

## 2.6 Effective material properties calculation

The thermoelectric materials properties are essential to design the system and this section represents the details and method which been studied and constructed by Elarusi et al. [13]. Determining the properties of thermoelectric materials is difficult and challenged for designers. Typically, some manufacturers provide only performance curves presenting values at constant junction temperature and that is not practical for designing thermoelectric systems. However, using the technique to find out these properties as well as the stand equations is effective and has high accuracy as they match the performance which is shown in the commercial module data sheet. To obtain these effective properties there are three parameters must be used which are: the maximum produced power can be generated by the selected module, maximum current, as well as maximum efficiency). Below are all the needed equations which are required to find out the module effective material properties. Equation (31) can be used to calculate the effective electrical resistivity, where $A_e$ is the cross section are of the module's single element, $L_e$ the length of the element, n number of thermocouples, the maximum power can be produced by the module is $W_{max}$ and $l_{max}$ is the maximum electrical current.

$$P_e = \frac{4(\frac{A_e}{L_e})W_{max}}{n(l_{max})^2} \tag{31}$$

In order to calculate the effective Seebeck coefficient the below equation 32 should be used, where $T_{hm}$ and $T_{cm}$ defined as the maximum and minimum operation temperatures of the module.

$$\alpha_e = \frac{4W_{max}}{n(I_{max})^2(T_{hm}-T_{cm})} \qquad (32)$$

The figure of merits can be calculated using equation 33, where $\eta_{max}$ is the module's maximum efficiency, and the average temperature $T_{avg} = \frac{(T_{hm}+T_{cm})}{2}$.

$$Z_e = \frac{\frac{2}{T_{avg}}(1+\frac{T_{cm}}{T_{hm}})}{(1-\frac{T_{cm}}{T_{hm}})\left(\frac{1}{\eta_{max}}+\frac{1}{2}\right)-2} \qquad (33)$$

To obtain the effective thermal conductivity the below equation 34 must be used, where $\alpha_e$ is Seebeck coefficient, $Z_e$ the figure merits, and $\rho_e$ is the electrical resistivity.

$$k_e = \frac{(\alpha_e)^2}{\rho_e Z_e} \qquad (34)$$

Hence, the above methodology explained the GTEG system in depth, where firstly the ideal equation of the GTEG system was formulated with some assumptions. Further, the first design of the proposed GTEG was explained where the thermal and electrical contact resistances were neglected and the used method and equations were presented without contact resistances. Furthermore, the second proposed design of the GTEG system was designed with different assumptions where the contact resistances were considered to study the effect of those contact as well as to help us for optimizing the proposed GTEG system. Finally, the three major components of the proposed GTEG system which are, heat sink, heat pipe, and the TEM module effective materials were

mentioned in details with all needed equations in order to design a proper GTEG system.

## 3   Results & Discussion:

### 3.1 Studying the accuracy of the proposed analytical design:

In order to study the current analytical design accuracy, the input data at the conducted experiment by Catalan. et al [14] has been applied to the current analytical design to study the accuracy of the used method. The commercial (Marlow - TG 12-8LS) module was used with the same specification, the input hot temperature of the geothermal to the system was 157℃ While the cold side ambient temperature was 17℃ . The hot side thermal resistance was 3.29 K/W and 0.16 K/W for the cold side thermal resistance. Figure 5 below shows the experimental design of Catalan .et al [14] which were studied the output power at three different cases with optimum value of the load resistance at 3.2 Ω. The first case they studied the output power at geothermal temperature of 200℃, the second case was at a temperature of 180℃, and 160℃ for the last case. Finally, the input data of Catalan. et al [14] were applied to the current proposed analytical design and then both results were compared as shown below in figure 6.
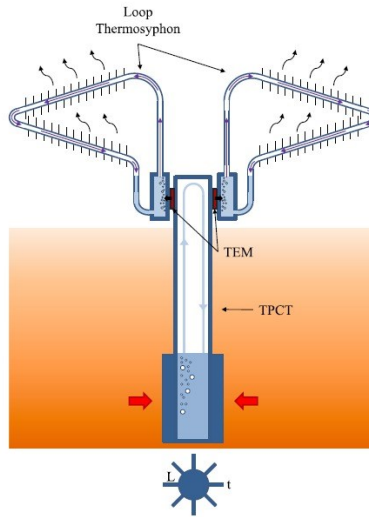
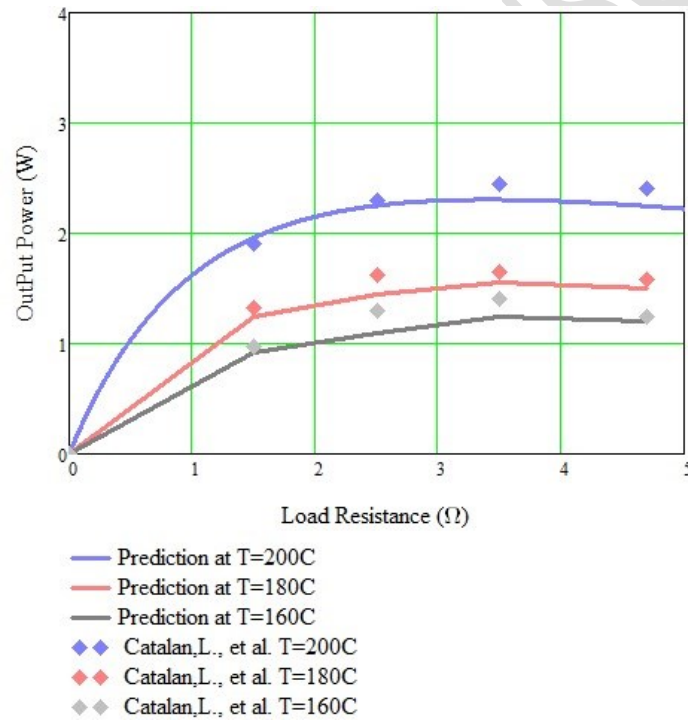**Figure 5:Experimental design of Catalan, L., et al. [14]**



**Figure 6: Comparison between the three different output power of the analytical design with Catalan. et al [14]**

**Table 2: The input parameters and effective material properties of the commercial selected module (Marlow - TG 12-8LS).**

| Input parameters | |
|---|---|
| n | 127 |
| $W_{max}$ | 7.95 W |

| | |
|---|---|
| $I_{max}$ | 3.38 A |
| $R_L$ | 2.49 Ω |
| $T_{hmax}$ | 230 ℃ |
| $T_{Cmax}$ | 50 ℃ |
| $A_e$ | $3.125\ mm^2$ |
| $L_e$ | 3.4 mm |
| $\eta_{mp}$ | 4.97% |
| ZT | 0.73 |
| **Obtained values** | |
| $k_e$ | 0.057 (W/cm. K) |
| $Z_e$ | $1.478.\ 10^{-3} (1/K)$ |
| $\rho_e$ | $2.014\ 10^{-3}\ (Ω.cm)$ |
| $\alpha_e$ | 411.561 (Mv/K) |

## 3.2 Results of design 1 the analytical proposed design neglecting contact residences:

The current study represents the proposed analytical design of GTEG system which aims to produce an electrical power by recovering the heat from geothermal source. In this section schematic diagrams and equations which been previously explained in the methodology section will be used again as they are, also heat pipe specifications, hot & cold temperatures which represent the geothermal and ambient temperatures, heat sink specification, effective material properties values and the selected commercial module specifications will be mentioned below in separate tables. Based on these values and parameters which were inserting into the previous mentioned equations which been addressed in the methodology section. The properties of both water and air were used at a temperature of 157℃ and 17 ℃. The maximum output electrical power of the system was obtained as 2.83 W per module at a load resistance values of 3.3 Ω and 3.4mm hight for the thermoelement leg length as well as the system power density was 0.144 W/cm^2.

**Table 3:The input parameters and specifications of the selected heat pipe and heat sinks for both designs.**

| The selected heat sink | Aluminum heat sinks |
|---|---|
| **Number of Fins** | **13** |
| **Fin Spacing** | **0.4 cm** |
| **Fin Thickness** | **0.3 cm** |
| **Thickness** | **4 cm** |
| **Length** | **4 cm** |
| **Profile Length** | **2 cm** |
| | |
| **The selected heat pipe** | **(ATS-HP-F6L400S11W-258)** |
| $L$ **(Heat Pipe Length)** | **40 cm** |
| $W$ **(Heat Pipe Width)** | **0.828 cm** |
| $H$ **(Heat Pipe Hight)** | **0.25 cm** |
| $n$ **(Number of Heat Pipes)** | **5** |
| $T_r$ **(Temperature Range)** | **30-120℃** |
| $W_F$ **(Filled Working Fluid)** | **Water** |

The above table 3 shows the selected commercial heat pipe and heat sink with their parameters and specifications which been used in the current proposed analytical design. A typical thermoelectric generator system must have a thermoelectric module connected to a heat exchanger system so that the maximum quantity of heat can be absorbed and released. Attaching a heat pipe to the hot side of the Thermoelectric generator module will assist to absorb as much heat as possible to the module, while placing a heat sink to the cold side of the TEG module will maximize the heat transfer rate by allowing it to release or discharge the maximum amount of heat into the environment. So, these two heat exchangers were selected and will be designed as per the method and equations mentioned in the methodology section 2.4 and 2.5.
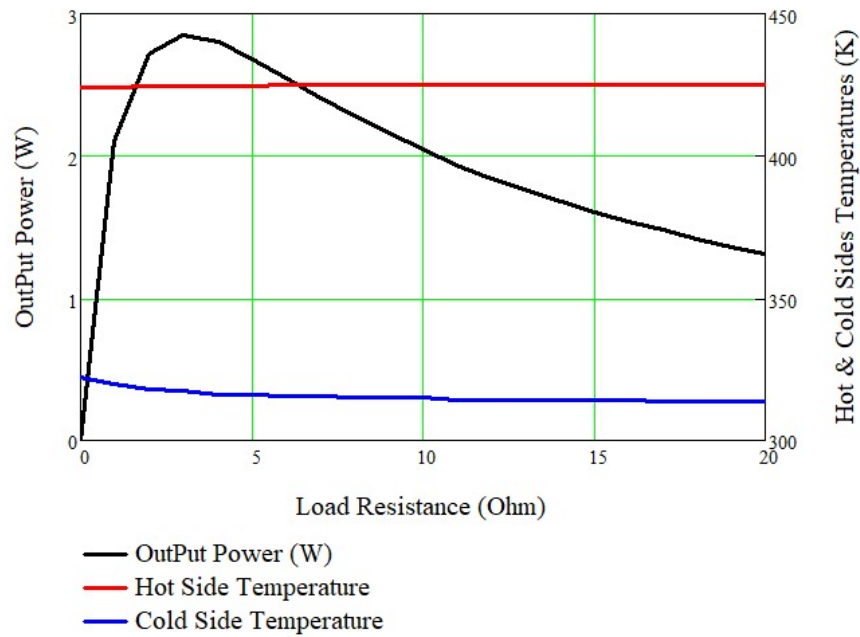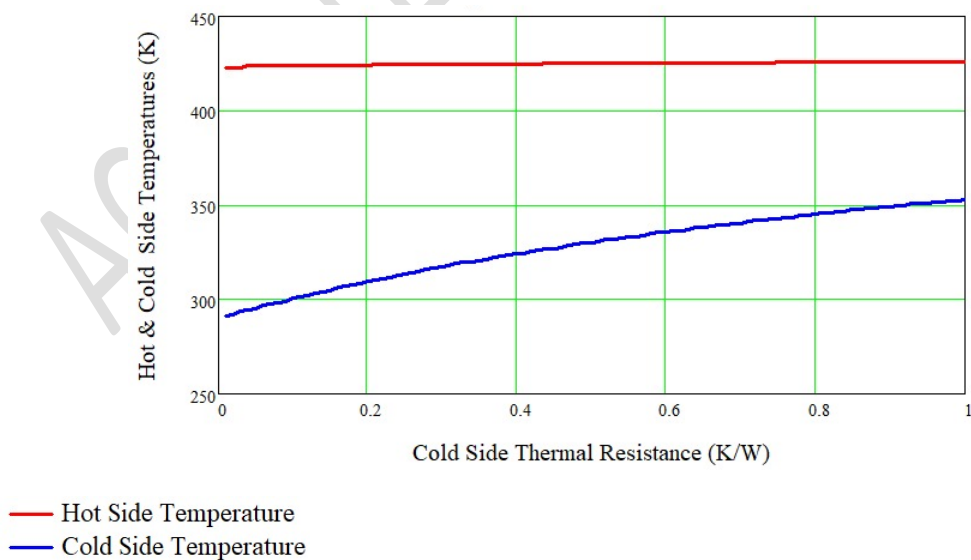
**Figure 7: Hot & Cold junction temperatures against electrical load resistance**

The above expression of figure 7 explains the relationship between both temperatures against the electrical load resistance. It can be seen that, how these two junction temperatures vary with load resistance, the hot junction temperature increases with increasing in load resistance value, while a reversible relation occurs with the cold side junction temperature.
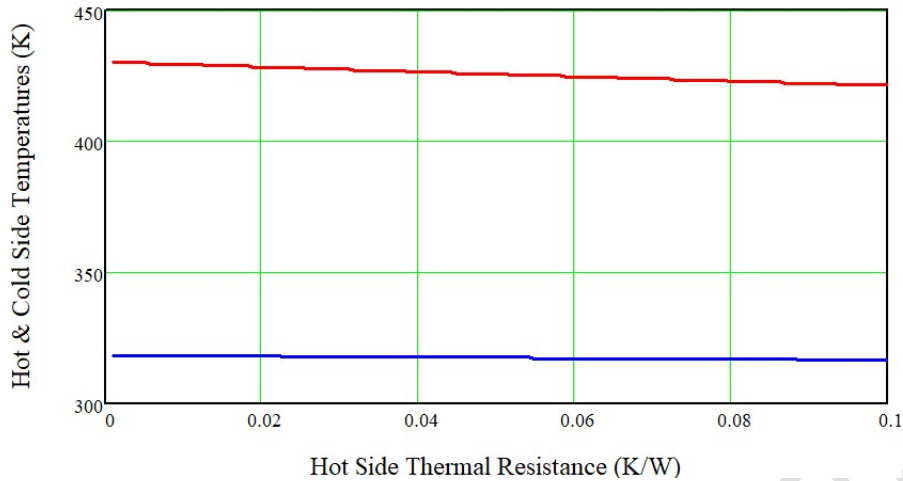


**(a)**

**Figure 8: (a) Hot & Cold junction temperatures versus cold fluid thermal Resistance and (b) Hot & Cold junction temperatures versus hot fluid thermal resistance**

— Hot Side Temperature
— Cold Side Temperature

**(b)**

Several parameters were used as an input to the system as been mentioned in the previous table 2. The number of thermoelements containing the module is 127 with a cross section area of 3.125 mm2 for a single thermoelement and the leg length Hight was 3.4mm. The module effective materials properties were also considered, the seebeck coefficient calculated as 411.561 Mv/K, the effective electrical resistivity value was 2.014 $10^{-3}$ Ω.cm, the figure of merits obtained as 1.478. $10^{-3}$ 1/K, and the effective thermal conductivity values was 0.057 W/cm. K. Furthermore, the temperature difference for the GTEG system is 140℃ where the input temperatures where the geothermal temperature which was 157℃ for the hot side and 17℃ for the cold side which represents the ambient temperature. As a result of the mentioned input parameters, figure 8 a & b explains how both temperatures react against the hot and cold thermal resistances which containing the system, it can be obviously notice that, increasing cold thermal resistance lead to a clear increase in the cold junction temperature and a little change in the hot junction temperature. While increasing the

25

hot side thermal resistance will decrease the junction temperature with a slight change in the cold junction temperature. However, the relationship between the power output and Hot fluid thermal resistance, and how these thermal resistances could affect on the output power. It can be noticed that smaller value of thermal resistances is always better for the system's output power as decreasing in thermal resistances lead to increasing in the power output.



**(a)**
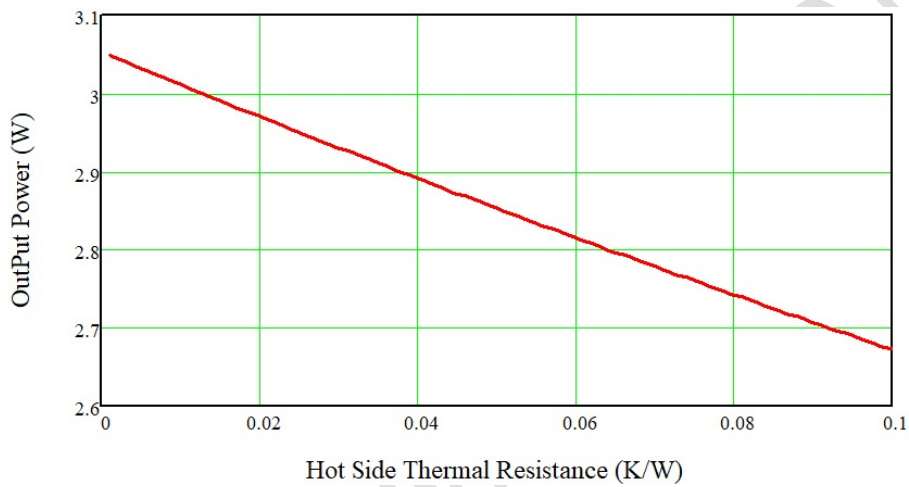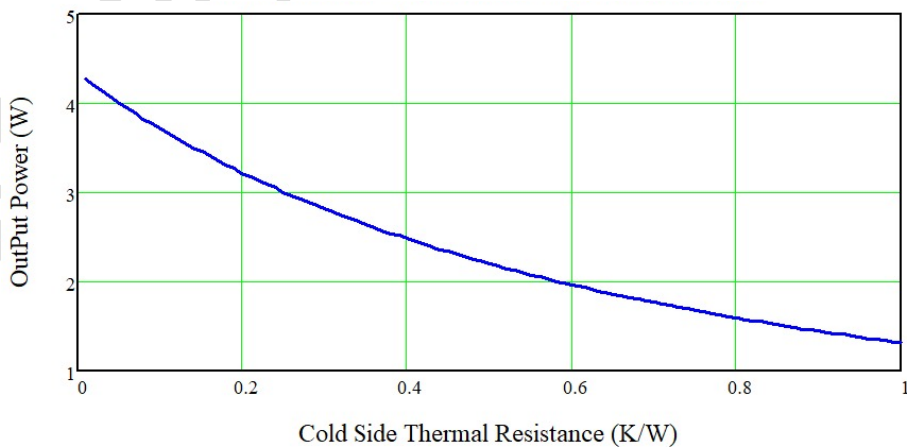


**Figure 9: System's output power versus (a) hot thermal resistance and (b) cold side thermal resistance for one module**

OutPut Power (W)

26

**(b)**

The above figures 9 (a) & (b) express how the system's thermal resistances could affect the output power, as it can be seen that, the relationship between the hot side thermal resistance and output power is a bit different than that of the cold side fluid. whereas, increasing the hot side thermal resistance will drop the output power highly compared with that of the cold side thermal resistance as increasing the cold side thermal resistance will gradually decrease the system output power. So, lower values of cold fluid thermal resistance lead to a higher output power, but the effect is lower than that of the hot fluid thermal resistance since the variation is gradually.

### 3.3  Results of GTEG design 2 including contact resistances:

The current study represents the proposed analytical design 2 of GTEG system which includes the contact resistance. The aim of design 2 is to optimize the first design by optimizing some parameters that could lead us to achieve the maximum possible output electrical power by recovering the heat from geothermal source. However, although there are several methods as per previous studies could be applied for optimizing the system, the method which been previously explained in section 2.3 will be used with the same input data and parameters which been used for design 1. So, the system will be designed again with considering contact resistances and the change of ceramic plate material, so that will show us the optimum value of the thermoelement leg length. Contact resistances are important parameters to be considered to study the thermoelectric materials performance and behavior. The following figure 10 show the change in output power versus load resistance when considering and including contact resistances.
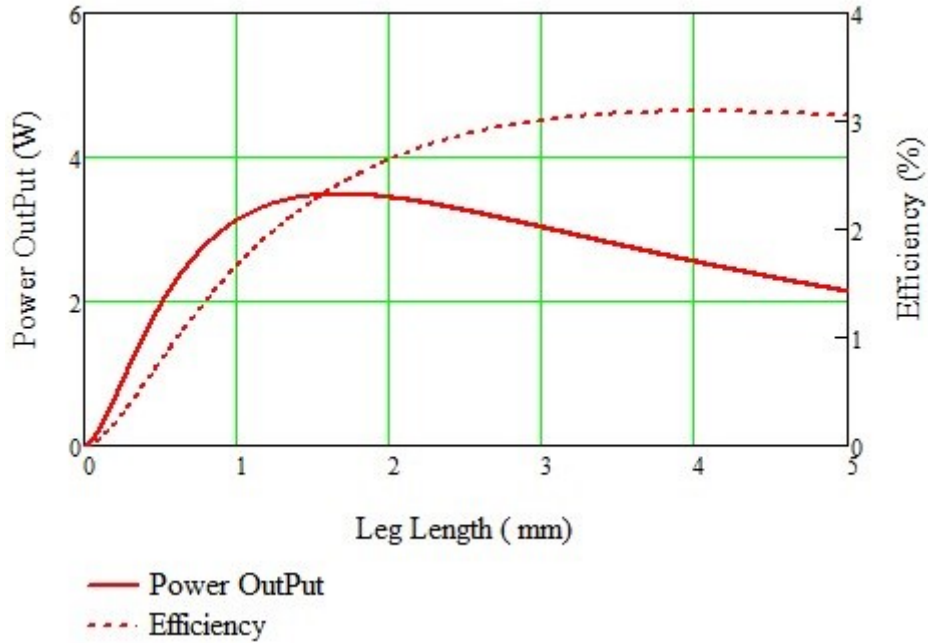
**Figure 10: The output power versus leg length**

The above figure 10 shows the output power versus the thermoelement leg length in three different cases, different material of the TEM ceramic plate and different thermoelement cross section area. The input hot temperature to the system was 157℃ and the ambient cold side temperature was 17℃, with 0.6 K/W thermal resistance for the hot side of the module and 0.3 K/W cold side thermal resistance. Furthermore, the load resistance value was 3.3 Ω and the thermoelement leg length is 3.4 mm. However, the above figure was obtained after using the previous mentioned input parameters, which shows the output power versus the thermoelement leg length in three different cases. The case which shows in a blue color represents the used thermoelectric module in the proposed analytical design. Thus, it can be clearly seen that, the optimum output power could be achieved at a leg length value of 1.8mm. However, this optimum value of leg length 1.8mm will be applied to the second proposed design to achieve the possible optimum output power.
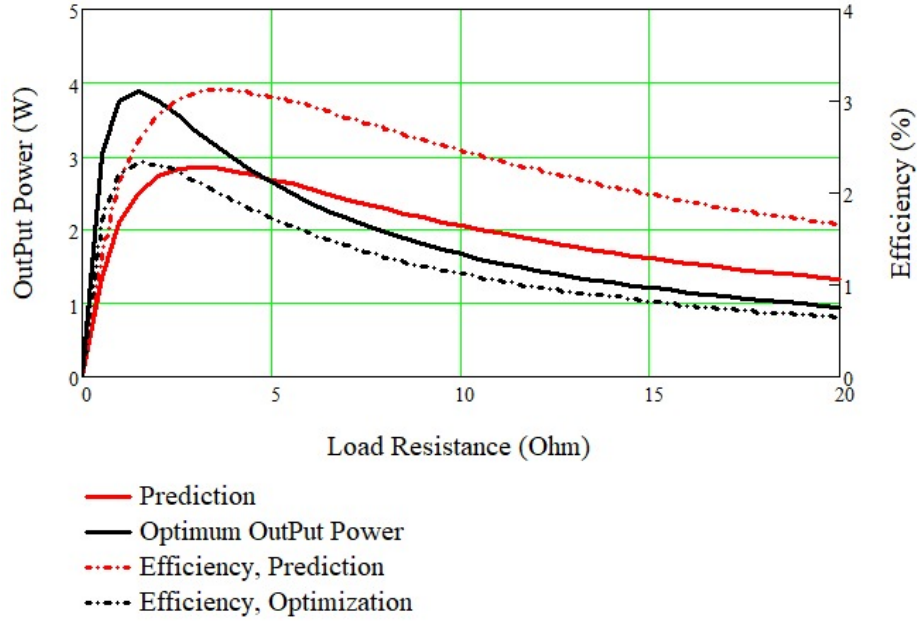
**Figure 11: System generated power & efficiency against load resistance**

Since the load resistance is needed to find out the produced power by the system, the above figure 11 shows the comparison and effect of the electrical load resistance upon the generated power of the system of both design 1 and 2. The figure also explains the relationship between the output power, conversion efficiency, and the load resistance as it shows the output power starts increasing with increasing in load resistance value until it reaches at a certain point which gives the maximum generated power of the system then the power starts decreasing with higher value of load resistance. The comparison between both designs could also be discussed, the input hot temperature to the system was 157℃ and cold side ambient temperature is 17℃ for both designs. The electrical output power of design 1 was 2.83 W with the load resistance value of 2.2 $\Omega$ and a leg length hight of 3.4mm while for the second design the load resistance was 2.2 $\Omega$ and 1.8mm leg length hight which improved the output power value by almost 34% from 2.83 W till 3.80 W which is the optimum value of the output electrical power.

**Table 4: The obtained results for the two proposed GTEG systems**

| Parameter | Design 1 (Neglecting contact resistances) ($Al_2O_3$) | Design 2 (Considering contact resistances) ($Al_2O_3$) |
|---|---|---|
| $T_h$ The Module's Hot Surface Temperature | 151.54 ℃ | 147.9 ℃ |
| $T_c$ The Module's Cold Surface Temperature | 43.46 ℃ | 61.5 ℃ |
| $T_g$ Geothermal Heat Temperature | 157 ℃ | 157 ℃ |
| $T_{amb}$ Ambient Temperature | 17℃ | 17 ℃ |
| $R_L$ Load Resistance | 3.3 Ω | 2.2 Ω |
| $L_e$ Leg length | 3.4 mm | 1.8 mm |
| $W_h$ Output Power | 2.83 W | 3.80 W |
| $P_d$ Power Density | 0.144 W/cm$^2$ | 0.235 W/cm$^2$ |

The shown results above in table 4 were obtained using the parameters and values which were presented in tables 2 and 3, with an optimum load resistance of 3.3 Ω, as well as the temperature difference was 140℃ where the input temperature of the system was 157℃ for the hot side and 17℃ the ambient air temperature.

## 4    Conclusion:

In conclusion, since the geothermal energy source is a huge field which also counted as one of the biggest sources of renewable energies, and thermoelectric generator technology has been suggested to accelerate the developments in geothermal power. Based on methods and techniques which been used in previous studies, this paper studied the new design of the GTEG system for geothermal heat recovery. However, the new proposed design of GTEG system aimed to recover the geothermal wasted energy and convert that wasted heat into usable electrical energy by using thermoelectric generator module. The proposed GTEG system was designed analytically using the methods which were explained in depth in the methodology section. The proposed GTEG system were designed twice, the first design was neglecting thermal and electrical contact resistances, while the second proposed designed was including the contact resistances in order to study the effect of these resistances among the system's performance. After that, the proposed analytical design was validated with Catalan experimental work in order to study the accuracy of our proposed GTEG design. However, both designs include two heat exchangers which are: heat pipe and heat sinks for hot and cold side, respectively. The effect of load resistance, heat sink, heat pipe, and number of thermoelements, were studied in depth in order to achieve the maximum output electrical power. The achieved output power density was 0.144 W/cm$^2$ under a temperature difference of 140℃ where the geothermal temperature was 157℃ which is the inlet temperature to the system, the ambient temperature was 17℃, and the module thermoelement leg length was 3.4mm. Finally, the proposed GTEG system was optimized by using the explained method in section 2.3 which lead to the result shown above in figure 10. Hence, the optimization method

was enhanced the power density by almost 35% where the optimum output power density archived as 0.235 W/cm$^2$.

## 5 References:

[1]. Catalan, L., et al., Field test of a geothermal thermoelectric generator without moving parts on the Hot Dry Rock field of Timanfaya National Park. Applied Thermal Engineering, 2023. 222: p. 119843.

[2]. Olasolo, P., et al., Enhanced geothermal systems (EGS): A review. Renewable and Sustainable Energy Reviews, 2016. 56: p. 133-144.

[3]. Catalan, L., et al., new opportunities for electricity generation in shallow hot dry rock fields: A study of thermoelectric generators with different heat exchangers. Energy Conversion and Management, 2019. 200: p. 112061.

[4]. Alegria, P., et al., Experimental development of a novel thermoelectric generator without moving parts to harness shallow hot dry rock fields. Applied Thermal Engineering, 2022. 200: p. 117619.

[5].Ahiska, R. and H. Mamur, Design and implementation of a new portable thermoelectric generator for low geothermal temperatures. IET Renewable Power Generation, 2013. 7(6): p. 700-706.

[6]. Alegría, P., et al., Design and optimization of thermoelectric generators for harnessing geothermal anomalies: A computational model and validation with experimental field results. Applied Thermal Engineering, 2024. 236: p. 121364.

[7]. Gavin Newsom, G., Thermoelectric Generator Application and Pilot Test in a Geothermal Field. 2022, California Energy Commission.

[8]. Bass, J.C.; Elsner, N.B.; Leavitt, F.A. Performance of the 1 kW thermoelectric generator for diesel engines. AIP Conf. Proc. 1994, 316, 295–298.

[9]. Birkholz, U.; Grob, E.; Stohrer, U.; Voss, K.; Gruden, D.; Wurster, W. Conversion of Waste Exhaust Heat in Automobile using FeSi2 Thermoelements. In Proceedings of the 7th International Conference on Thermoelectric Energy Conversion, Arlington, TX, USA, 16–18 March 1988; pp. 124–128.

[10]. Attar, A., Lee, H. and Snyder, G.J., 2020. Optimum load resistance for a thermoelectric generator system. Energy Conversion and Management, 226, p.113490.

[11]. Weera, S., Lee, H. and Attar, A., 2020. Utilizing effective material properties to validate the performance of thermoelectric cooler and generator modules. Energy Conversion and Management, 205, p.112427.

[12]. H. Lee, Thermal Design: Heat Sinks, Thermoelectric, Heat Pipes, Compact Heat Exchangers, and Solar Cells, Hoboken: John Wiley & Sons, Inc., 2010.

[13]. Abdul Elarusi, Hassan Fagehi, Alaa Attar, HoSung Lee, "Theoretical Approach to Predict the Performance of Thermoelectric Generator Modules, " Journal of Electronic Materials, vol. accepted, 2016.

[14]. Catalan, L., et al., Computational study of geothermal thermoelectric generators with phase change heat exchangers. Energy Conversion and Management, 2020. 221: p. 113120.